Constructing the GGE in integrable models: A Hilbert space Monte Carlo approach

Vincenzo Alba[1] and Maurizio Fagotti[2]

[1]*International School for Advanced Studies (SISSA), Via Bonomea 265, 34136, Trieste, Italy, INFN, Sezione di Trieste*
[2]*Département de Physique, Ecole normale superieure, CNRS, 24 rue Lhomond, 75005 Paris, France*

(Dated: June 30, 2015)

I. INTRODUCTION

The issue of how statistical ensembles emerge from the out-of-equilibrium unitary dynamics in isolated quantum many-body system is a fundamental, yet still challenging, problem. Much of the motivation for the renewed interest in this topic originated from the possibility of simulating efficiently the out-of-equilibrium dynamics in cold atom experiments. The paradigm of out-of-equilibrium experiment is the quantum quench, in which

In a generic *global* quench in an isolated quantum many-body system let us consider the initial state $|\Psi_0\rangle$. In the thermodynamic limit for generic $|\Psi_0\rangle$ the system is expected to equilibrate. The most relevant question is whether expectation values of observables can be computed in a thermodynamic ensemble.

Moreover, in integrable models the out-of-equilibrium dynamics is strongly affected by the presence of non-trivial local integral of motion.

It is believed that the equilibrium expectation values of local operators at long times are described by a Generalized Gibbs Ensemble (GGE). More quantitatively,

$$\lim_{t\to\infty}\lim_{L\to\infty}\langle\Psi(t)|\mathcal{O}|\Psi(t)\rangle=\langle\mathcal{O}\rangle_{GGE}, \tag{1}$$

with

$$\langle\mathcal{O}\rangle_{GGE}\equiv\lim_{L\to\infty}\frac{\mathrm{Tr}(\mathcal{O}\rho^{GGE})}{\mathrm{Tr}(\rho^{GGE})}. \tag{2}$$

with L being the system size. The GGE density matrix ρ^{GGE} is defined as

$$\rho^{GGE}=\lim_{\mathcal{N}\to\infty}\frac{1}{Z}\exp\Big(-\sum_{j=1}^{\mathcal{N}}\lambda_j\mathcal{I}_j\Big) \tag{3}$$

where Z is the normalization, $\mathcal{I}_j$ the integral of motion, λ_j the associated Lagrange multipliers. These are determined by imposing that $\langle\Psi_0|\mathcal{I}_j|\Psi_0\rangle=\langle\mathcal{O}\rangle_{GGE}$.

We provide a Monte Carlo method to simulate the GGE statistica ensemble.

Remarkably, this allows to extract the rapidity densities defining the ensemble representative state in the thermodynamic limit.

Notice these are related to the momentum distribution functions of the steady state routinely measured in cold atom experiments.

Finite-size effects are under control and for moderately large chain sizes the Monte Carlo results agree very well with the thermodynamic limit results, especially for small rapidities. Higher rapidities are more sensitive to finite size effects as they reflec short length scales.

The method allows to address local observables for which the expression in terms of the rapidity is known as well.

An alternative numerical method would be Quantum Monte Carlo. However, this would require the implementation of the higher conserved charges, other than the Hamiltonian. As the range of higher charges becomes large this is not easily doable in practice.

We provide the first numerical verification of the validity of the GTBA equations for the Heisenberg spin chain.

Interestingly, finite-size corrections are generically small, i.e., expontially decaying with the chain size.

Our Monte Carlo approach can be trivially extended to include other conserved charges, both local and non-local, and arbitrary functions of the rapidities. While the former is related to the GGE average of the particle number, the latter measures its fluctuations. Notice that due to the $SU(2)$ symmetry of the conserved charges one has that $\langle S_z\rangle=0$ (panel (g)).

II. THE HEISENBERG SPIN CHAIN

The isotropic spin-$\frac{1}{2}$ Heisenberg (XXX) chain is defined by the Hamiltonian

$$\mathcal{H}\equiv J\sum_{i=1}^{L}\left[\frac{1}{2}(S_i^+S_{i+1}^-+S_i^-S_{i+1}^+)+S_i^zS_{i+1}^z\right], \tag{4}$$

where $S_i^\pm\equiv(\sigma_i^x\pm i\sigma_i^y)/2$ are spin operators acting on the site i of the chain, $S_i^z\equiv\sigma_i^z/2$, and $\sigma_i^{x,y,z}$ the Pauli matrices. We fix $J=1$ and use periodic boundary conditions identifying sites $L+1$ and 1. The total magnetization $S_T^z\equiv\sum_i S_i^z=L/2-M$, with M number of down spins (particles), commute with (4). Thus, the eigenstates of (4) can be labelled by M.

In the Bethe ansatz framework each eigenstate of (4) is univocally identified by a set of M complex parameters (so-called rapidities) $\{x_\alpha\in\mathbb{C}\}_{\alpha=1}^M$. In the thermodynamic limit $L\to\infty$ the rapidities x_α form "string" patterns along the imaginary direction in the complex plane (string hypothesis). The rapidities forming a string of length $1\le n\le M$ (so-called n-string) are parametrized as $x_\gamma^{(n,j)}=x_\gamma^{(n)}-i(n-1-2j)$, $\quad j=0,1,\dots,n-1$,, where $x_{n;\gamma}\in\mathbb{R}$ is the real part of the string (string center), j labels the different rapidities in the same n-string, andγ denotes strings of the same length but with different centers. Although the string hypothesis is not correct for finite chains, deviations typically, i.e., for most

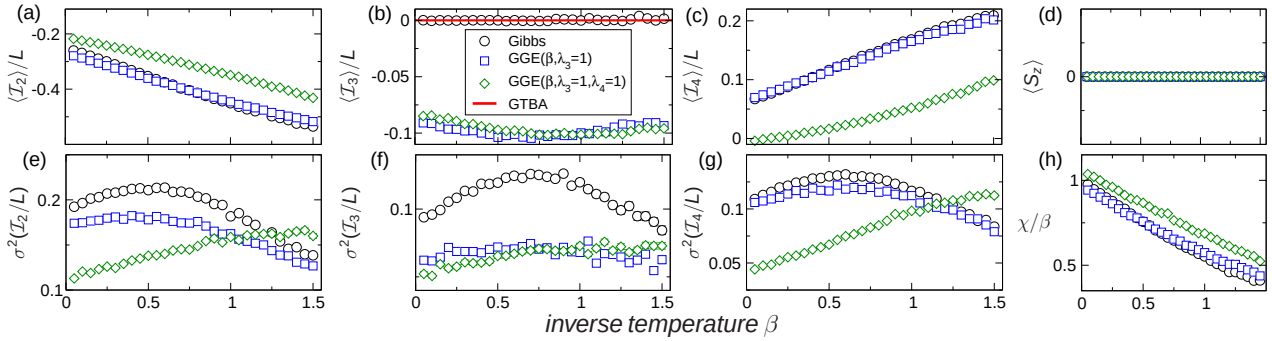

FIG. 1. The Generalized Gibbs Ensemble (GGE) for the Heisenberg spin chain with $L = 16$ sites: numerical results obtained using the Hilbert space Monte Carlo sampling. Only the first three conserved charges $\mathcal{I}_n$ ($n = 1, 2, 3$), with associated Lagrange multipliers λ_n, are included in the GGE. Here $\mathcal{I}_2$ is the Hamiltonian and $\lambda_2 \equiv \beta$ the inverse temperature. In all the panels different symbols correspond to different values of λ_3, λ_4. The circles correspond to the Gibbs ensemble, i.e., $\lambda_3 = \lambda_4 = 0$. (a) The GGE average $\langle \mathcal{I}_2/L \rangle$ plotted as a function of β. (b) Variance of the GGE fluctuations $\sigma^2(\mathcal{I}_2/L) \equiv \langle (\mathcal{I}_2/L)^2 \rangle - \langle \mathcal{I}_2/L \rangle^2$ as a function of β. (c)(d) and (e)(f): Same as in (a)(b) for $\mathcal{I}_3$ and $\mathcal{I}_4$, respectively. In all panels the dash-dotted lines are the analytical results obtained using the Generalized Thermodynamic Bethe Ansatz (GTBA). (g) The GGE expectation value of the total magnetization $\langle S_z \rangle$. Notice that $\langle S_z \rangle = 0$ due to the $SU(2)$ invariance of the conserved charges. (h) χ/β plotted versus β, with χ being the magnetic susceptibility per site.

of the eigenstates, decay exponentially with system size. The string centers $x_{n;\gamma}$ are solutions of the Bethe-Takahashi equations

$$L\vartheta_n(x_{n;\gamma}) = 2\pi I_{n;\gamma} + \sum_{(m,\beta)\neq(n,\gamma)} \Theta_{m,n}(x_{n;\gamma} - x_{m;\beta}). \quad (5)$$

Here $\vartheta_n(x) \equiv 2\arctan(x/n)$, $\Theta_{m,n}(x)$ is the scattering phase between different rapidities, and $I_{n;\gamma} \in \frac{1}{2}\mathbb{Z}$ are the so-called Bethe-Takahashi quantum numbers. The $I_{n;\gamma}$ obey the upper bound $|I_{n;\gamma}| \leq I_{\rm MAX}(n, L, M)$, with $I_{\rm MAX}$ a known function of n, M, L. Every choice of $I_{n;\gamma}$ identifies an eigenstate of (4). Notice that each eigenstate contains strings of different lengths. We define the "string content" of an eigenstate as $\mathcal{S} \equiv \{s_1, \ldots, s_M\}$, with $0 \leq s_n \leq \lfloor M/n \rfloor$ the number of n-strings. By definition one has $\sum_j j s_j = M$.

Besides the total magnetization and the momentum, the XXX chain has non-trivial *local* conserved charges $\mathcal{I}_j$, with $[\mathcal{I}_j, \mathcal{I}_k] = 0 \, \forall j, k$. These are obtained as

$$\mathcal{I}_{j+1} \equiv \frac{i}{(j-1)!} \frac{d^j}{dy^j} \log(\Lambda(\{x_{n;\gamma}\}, y))\Big|_{y=i}. \quad (6)$$

Here Λ in the Algebraic Bethe ansatz is the eigenvalue of the quantum transfer matrix $T(y)$, with y the spectral parameter. The dependence of Λ on the rapidities $x_{n;\gamma}$ is known. One can check that $\mathcal{I}_2 = \mathcal{H}$. The range of $\mathcal{I}_j$ increases linearly with j, i.e., larger j correspond to less local charges. Remarkably, the eigenvalues of $\mathcal{I}_j$ over a generic eigenstate are obtained by summing the contributions of the different string sectors independently. For instance, the energy is obtained as $E = \sum_n E_n$, where $E_n = 2\sum_\gamma n/(n^2 + x_{n;\gamma}^2)$.

III. HILBERT SPACE MONTE CARLO SAMPLING

For a finite chain the GGE ensemble can be generated by sampling the eigenstates of (4) with the probability (3). This can be done efficiently using Monte Carlo. One starts with an initial M particle eigenstate of (4), with string content $\mathcal{S} = \{s_1, \ldots, s_M\}$, identified by Bethe-Takahashi quantum number configuration $\mathcal{C} = \{I_{n;\gamma}\}_{n=1}^{M}$ ($\gamma = 1, \ldots, s_n$). Let us denote the expectation values of the conserved charges as $\{\mathcal{I}_j\}$. The basic idea is to generate a new eigenstate with a Metropolis update. Specifically, each Monte Carlo step (mcs) consists of three moves:

1. Choose a new particle number sector M' and a string content $\mathcal{S}'$ with probability $P(M', \mathcal{S}')$.

2. Generate a quantum number configuration $\mathcal{C}'$ compatible with the $\mathcal{S}'$ obtained in step 1 and solve the Bethe-Takahashi equations (5) to extract the new rapidities $\{x_{n;\gamma}\}$.

3. After calculating the expctation values of the charges $\mathcal{I}'_j$ accept the new eigenstate with the Metropolis probability:

$$\text{Min}\left(1, \frac{L - 2M' + 1}{L - 2M + 1} e^{-\sum_j \lambda_j (\mathcal{I}'_j - \mathcal{I}_j)}\right). \quad (7)$$

In (7) the factor in fron of the exponential takes into account that eigenstates in the same $SU(2)$ mutliplet have the same charges expectation value, i.e., the $\mathcal{I}_j$ are $SU(2)$ scalars. Crucially, the steps 1 and 2 are necessary in order to account for the density of states of the Heisenberg spin chain. The Markov chain defined by the steps $1-3$, after a thermalization, generates eigenstates sampled according to (3). We should mention that a similar method has been developed in Ref... to construct the the Gibbs ensemble in the Heisenberg spin chain.

The GGE expectation values $\langle \mathcal{O} \rangle$ are as the average of the expectation values of $\mathcal{O}$ over the eigenstates $|\{x_{n;\gamma}\}\rangle$ generated by the Monte Carlo as

$$\langle \mathcal{O} \rangle = \frac{1}{N_{\rm mcs}} \sum_{\{x_{n;\gamma}\}} \langle \{x_{n;\gamma}\} | \mathcal{O} | \{x_{n;\gamma}\} \rangle, \quad (8)$$

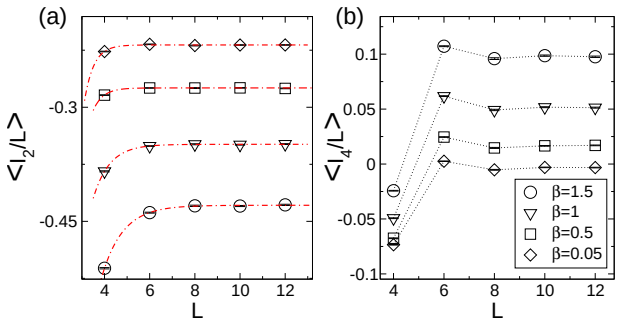

FIG. 2. Finite-size scaling of the GGE averages in the Heisenberg chain: Numerical results obtained from the Hilbert space Monte Carlo sampling. Here the GGE is constructed including $\mathcal{I}_2, \mathcal{I}_3, \mathcal{I}_4$, with Lagrange multipliers $\lambda_2 = \beta, \lambda_3 = \lambda_4 = 1$. (a) $\langle \mathcal{I}_2/L \rangle$ plotted versus the chain size L for several values of β. The dash-dotted lines are exponential fits. (b) Same as in (a) for $\mathcal{I}_4$.

where $N_{\rm mcs}$ is the number of Monte Carlo steps.

IV. GGE FOR LOCAL OBSERVABLES

The validity of the Monte Carlo method is illustrated in Fig. 3 considering the GGE expectation values of the charge densities $\langle \mathcal{I}_j/L \rangle$ (panels (a)-(c) in the Figure) and the variance of their ensemble fluctuations $\sigma^2(\mathcal{I}_j) \equiv \langle \mathcal{I}_j^2 \rangle - \langle \mathcal{I}_j \rangle^2$ (panels (d)-(f)). Finally, panels (g)(h) plot the total magnetization $\langle S_z \rangle$ (i.e., the particle number) and the spin susceptibility χ (particle number fluctutations). Notice that $\sigma^2(\mathcal{I}_2)$ is related to the specific heat, $\mathcal{I}_3 \equiv \sum_{\alpha\beta\gamma} \epsilon_{\alpha\beta\gamma} \sigma_i^\beta \sigma_{i+1}^\gamma \sigma_{i+2}^\alpha$ is the energy current, and $\sigma^2(\mathcal{I}_3)$ is related to the energy Drude weight. Here the data are for the truncated TGGE constructed with the first three charges $\mathcal{I}_2, \mathcal{I}_3, \mathcal{I}_4$. We consider several values of the Lagrange multipliers, namely $\lambda_3 = \lambda_4 = 0$ (Gibbs ensemble, circles in the Figure), $\lambda_3 = 1$ and $\lambda_4 = 0$ (squares), and $\lambda_3 = \lambda_4 = 1$ (rhombi). All our results are plotted versus the inverse temperature $\lambda_2 = \beta$. The data are Monte Carlo results for $N_{\rm mcs} = 5 \cdot 10^5$. In most of the cases, especially for small β the Monte Carlo error bars are small than the symbols. As expected, the different ensemble give different expectation values, implying that the local observables we consider are able to distinguish different GGEs. Notice that in panel (b) $\langle \mathcal{I}_3 \rangle = 0$ for the Gibbs ensemble due to the parity invariance of $\mathcal{I}_j$ with even j, while in (d) $\langle S_z \rangle = 0$ due to the $SU(2)$ symmetry of (4). In all the panels in Fig. 3 the continuous lines are the analyitic results obtained in the thermodynamic limit by solving the $GTBA$ equations. These which fully match the Monte Carlo data, which signals that the finite-size effects are negligible already for $L = 16$, at least for the values of the λ_j considered.

The finite-size corrections are more carefully investigated in Fig. 2. Fig. 2 plots $\langle \mathcal{I}_2 \rangle$ and $\langle \mathcal{I}_4 \rangle$ (panels (a) and (b), respectively) versus β. Here we focus on the $TGGE$ with $\lambda_2 = \beta, \lambda_3 = 0$ and $\lambda_4 = 1$. Panel (a) demonstrates that finite-size effects decay exponentially with L for any β. Clearly, corrections are larger at lower temperature, as expected. Moreover, they increase with the range of the operator as shown in panel (b), although the behavior remains exponential.

V. EXTRACTING THE RAPIDITY DENSITIES

For a generic observable $\mathcal{O}$ in the thermodynamic limit the GGE expectation value become a functional integral over the root distributions $\rho_n(x)$ as

$$\sum_{\text{eigenstates}} \mathcal{O} \exp\left(\sum_j \lambda_j \mathcal{I}_j\right) \to \int \mathcal{D}\boldsymbol{\rho} \exp\left(S_{YY}[\boldsymbol{\rho}]\right) \quad (9)$$

The rapidity densities ρ_n^p of the ensemble representative state can be measured in Monte Carlo from the histograms of the roots generated in the Monte Carlo history.

This is illustrated in Fig. 3 for several ensembles. In the Figure panels (a)-(c) plot the first three root densities $\rho_n(x)$ for $n = 1, 2, 3$ as a function of x for the representative state of the infinite-temperature Gibbs ensemble. We restrict ourselves to the interval $-6 \leq x \leq 6$. In each panel the different histograms correspond to different chain sizes $18 \leq L \leq 30$. The histograms are obtained from $4 \cdot 10^5$ Monte Carlo steps. The width of the histogram bins is given as $2/L$. In all the panels the full lines are the analytic results obtained from the Thermodynamic Bethe Ansatz (TBA) (cf. (16)). Remarkably, although finite-size effects are present, the Monte Carlo data are in good agreement with the TBA results. This is especially true for ρ_1, whereas finite-size corrections become progressively worse upon considering larger $n > 1$ (see panels (b)(c)). Clearly, these corrections are vanishing upon increasing the system size (see for instance the arrow in panel (b)). Moreover, the finite size effects become larger upon increasing the rapidity x. This is expected as larger rapidity correspond to larger quasi-momenta, which are more sensitive to the lattice effects. Finally, finite-size effects increase with n. This is somewhat expected since larger n correspond to more extended many-spin bound states.

Finite-temperature ensemble can be also considered. This is illustrated in panel (g) discussing the Gibbs ensemble at inverse temperature $\beta = 1/2$ and $\beta = 1$ (different histograms in the panel). We focus on $\rho_1(x)$ The data for infinite temperature are reported for comparison. All the histograms are obtained for $L = 30$. The full lines are now the analytic results obtained by solving the TBA equations and perfectly agree with the Monte Carlo data. Notice that upon lowering the temperature the height of the zero rapidity peak increases. This reflects that at $T = 0$ the ground state of the antiferromagnetic Heisenberg chain are packed around $x = 0$, and the contribution of nonzero rapidity is vanishing exponentially.

Finally, in panels (d)(f) we present the rapidity densities $\rho_n(x)$ for the GGE ensemble. Specifically, here we focus on the GGE obtained including the two charges $\mathcal{I}_2$ and $\mathcal{I}_4$. We fix the associated Lagrange multipliers to $\lambda_2 = 0$ and $\lambda_4 = 1$. Similar to the Gibbs ensemble, panels (a)(c) suggest that for $L = 30$ the finite size effects are negligible, at least in the interval $-2 \leq x \leq 2$.

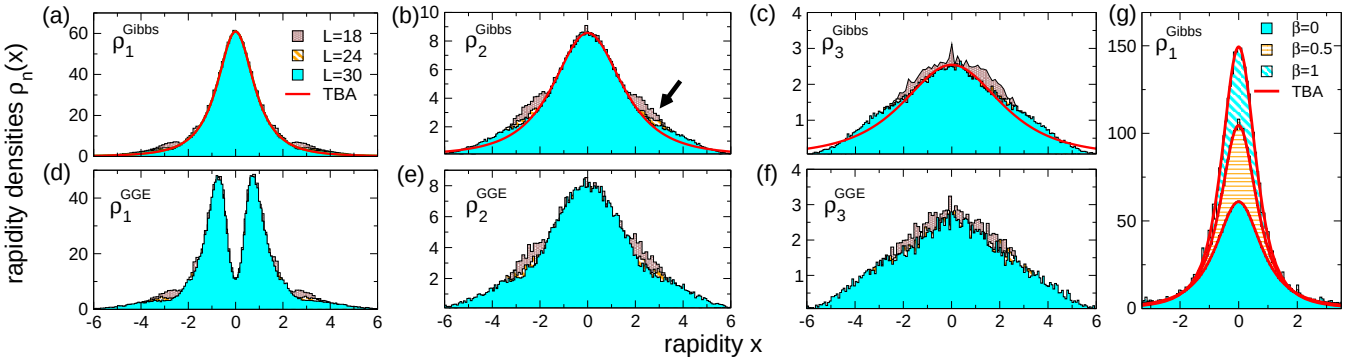

FIG. 3. The rapidity densities $\rho_n(x)$ (for $n = 1, 2, 3$) for the infinite temperature Gibbs (panels (a)-(c)) and the GGE equilibrium states (panels (d)-(f)): Numerical results for the Heisenberg spin chain obtained using the Hilbert space Monte Carlo sampling. Here the GGE is constructed including only $\mathcal{I}_2$ and $\mathcal{I}_4$ with fixed Lagrange multipliers $\lambda_2 = 0$ and $\lambda_4 = 1$. In all the panels the data are the histograms of the n-strings rapidities sampled in the Monte Carlo. The width of the histogram bins is $\Delta x = 2/L$. In each panel different histograms correspond to different chain sizes L. All the histograms are divided by 10^3 for convenience. In (b) the arrow is to highlight the finite-size effects. In panels (a)-(c) the lines are the Thermodynamic Bethe Ansatz (TBA) results. (g) Finite-temperature effects: Monte Carlo data for ρ_1^{Gibbs} for different values of the inverse temperature β.

A. The thermodynamic limit

In the thermodynamic limit, i.e., for $L \to \infty$ the Bethe eigenstates are described by the distributions of the string centers ρ_n. These are defined such that $L\rho_n(x)$ gives the number of n-strings in the interval $[x, x + dx]$. More formally $\rho_n^p(x)$ can be defined as

$$\rho_n^p(x) \equiv \frac{1}{L(x_{\gamma+1}^{(n)} - x_\gamma^{(n)})} \tag{10}$$

The Bethe-Takahashi equations (5) are replaced by the integral equations

$$\rho_n^p(x) + \rho_n^h(x) = a_n(x) + \sum_{m=1}^{\infty} a_{nm} \rho_m^p(x) \tag{11}$$

Moreover, sum over eigenstates can be replaced by

$$\sum_{\text{states}} \to \int \mathcal{D}\boldsymbol{\rho}^p e^{S_{YY}[\boldsymbol{\rho}^p]}, \tag{12}$$

where $\boldsymbol{\rho}^p \equiv \{\rho_n^p\}_{n=1}^{\infty}$, and $S_{YY}[\boldsymbol{\rho}]$ is the Yang-Yang entropy

$$S_{YY}[\boldsymbol{\rho}] \equiv N \sum_{n=1}^{\infty} \int_{-\infty}^{+\infty} \rho_n(x) \log\left(1 + \frac{\rho_n^h(x)}{\rho_n(x)}\right) + \rho_n^h \log\left(1 + \frac{\rho_n(x)}{\rho_n^h(x)}\right). \tag{13}$$

The Yang-Yang entropy counts the number of eigenstates that in the thermodynamic limit lead to the same $\boldsymbol{\rho}$.

VI. THE STRING ROOT DENSITIES AT INFINITE TEMPERATURE

For infinite temperature the densities ρ_n are given as

$$\rho_n(x) = \frac{2}{\pi} \frac{1}{(n^2 + x^2)(x^2 + (2+n)^2)} \tag{14}$$

Notice that

$$\int_{-\infty}^{+\infty} \rho_n(x) dx = \frac{1}{n(n+1)(n+2)} \tag{15}$$

Icluding the first order correction to the infinite temperature result one obtains

$$\rho_n(x) = \frac{2}{\pi} \frac{1}{(n^2 + x^2)(x^2 + (2+n)^2)} - \frac{8}{\pi} \frac{n(n+2)}{(n^2 + x^2)^2 (x^2 + (2+n)^2)^2} J\beta + \mathcal{O}(J^2\beta^2) \tag{16}$$

[1] M. Rigol, V. Dunjko, V. Yurovsky, and M. Olshanii, Phys. Rev. Lett. **98**, 050405 (2007).
[2] S. Popescu, A. J. Short, and A. Winter, Nature Physics **2**, 754 (2006).
[3] M. Rigol, V. Dunjko, and M. Olshanii, Nature **452**, 854 (2008).
[4] A. Polkovnikov, K. Sengupta, and M. Vengalattore, Rev. Mod. Phys. **83**, 863 (2011).
[5] J. Eisert., M. Friesdorf, and C. Gogolin, arXiv:1408.5148.
[6] C. Kollath, A. M. Läuchli, and E. Altman, Phys. Rev. Lett. **98**, 180601 (2007).

[7] S. R. Manmana, S. Wessel, R. M. Noack, and A. Muramatsu, Phys. Rev. Lett. **98**, 210405 (2007).
[8] P. Calabrese and J. Cardy, J. Stat. Mech. P06008 (2007).
[9] M. Cramer, C. M. Dawson, J. Eisert, and T. J. Osborne, Phys. Rev. Lett. **100**, 030602 (2008).
[10] T. Barthel and U. Schollwöck, Phys. Rev. Lett. **100**, 100601 (2008).
[11] M. Cramer, A. Flesch, I. P. McCulloch, U. Schollwöck, and J. Eisert, Phys. Rev. Lett. **101**, 063001 (2008).
[12] M. Kollar and M. Eckstein, Phys. Rev. A **78**, 013626 (2008).
[13] A. Iucci and M. A. Cazalilla, Phys. Rev. A **80**, 063619 (2009).
[14] S. Sotiriadis, P. Calabrese, and J. Cardy, EPL **87**, 20002 (2009).
[15] G. Roux, Phys. Rev. A **79**, 021608 (2009).
[16] M. Rigol, Phys. Rev. Lett. **103**, 100403 (2009).
[17] M. Rigol, Phys. Rev. A **80**, 053607 (2009).
[18] P. Barmettler, M. Punk, V. Gritsev, E. Demler, and E. Altman, Phys. Rev. Lett. **102**, 130603 (2009).
[19] P. Barmettler, M. Punk, V. Gritsev, E. Demler, and E. Altman, New J. Phys. **12**, 055017 (2010).
[20] M. Cramer and J. Eisert, New J. Phys. **12**, 055020 (2010).
[21] A. Flesch, M. Cramer, I. P. McCulloch, U. Schollwöck, and J. Eisert, Phys. Rev. A **78**, 033608 (2008).
[22] G. Roux, Phys. Rev. A **81**, 053604 (2010).
[23] D. Fioretto and G. Mussardo, New J. Phys. **12**, 055015 (2010).
[24] G. Biroli, C. Kollath, and A. M. Läuchli, Phys. Rev. Lett. **105**, 250401 (2010).
[25] L. F. Santos and M. Rigol, Phys. Rev. E **82**, 031130 (2010).
[26] M. C. Bañuls, J. I. Cirac, and M. B. Hastings, Phys. Rev. Lett. **106**, 050405 (2011).
[27] P. Calabrese, F. H. L. Essler, and M. Fagotti, Phys. Rev. Lett. **106**, 227203 (2011).
[28] C. Gogolin, M. P. Mueller, and J. Eisert, Phys. Rev. Lett. **106**, 040401 (2011).
[29] M. Rigol and M. Fitzpatrick, Phys. Rev. A **84**, 033640 (2011).
[30] T. Caneva, E. Canovi, D. Rossini, G. E. Santoro, and A. Silva, J. Stat. Mech. (2011) P07015.
[31] L. Santos, A. Polkovnikov, and M. Rigol, Phys. Rev. Lett. **107**, 040601 (2011).
[32] A. C. Cassidy, C. W. Clark, and M. Rigol, Phys. Rev. Lett. **106**, 140405 (2011).
[33] F. H. L. Essler, S. Evangelisti, and M. Fagotti, Phys. Rev. Lett. **109**, 247206 (2012).
[34] M. A. Cazalilla, A. Iucci, and M.-C. Chung, Phys. Rev. E **85**, 011133 (2012).
[35] J. Mossel and J.-S. Caux, New J. Phys. **14** 075006 (2012).
[36] M. Rigol and M. Srednicki, Phys. Rev. Lett. **108**, 110601 (2012).
[37] J. Mossel and J.-S. Caux, J. Phys. A: Math. Theor. **45**, 255001 (2012).
[38] M. Fagotti and F. H. L. Essler, Phys. Rev. B **87**, 245107 (2013).
[39] M. Fagotti, Phys. Rev. B **87**, 165106 (2013).
[40] M. Collura, S. Sotiriadis, and P. Calabrese, Phys. Rev. Lett. **110**, 245301 (2013).
[41] J.-S. Caux and F. H. L. Essler, Phys. Rev. Lett. **110**, 257203 (2013).
[42] M. Kormos, A. Shashi, Y.-Z. Chou, J.-S. Caux, and A. Imambekov, Phys. Rev. B **88**, 205131 (2013).
[43] B. Bertini, D. Schuricht, and F. H. L. Essler, arXiv:1405.4813 (2014).
[44] S. Sotiriadis and P. Calabrese, J. Stat. Mech. (2014) P07024.
[45] F. H. L. Essler, S. Kehrein, S. R. Manmana, and N. J. Robinson, Phys. Rev. B **89**, 165104 (2014).
[46] M. Fagotti, M. Collura, F. H. L. Essler, and P. Calabrese, Phys. Rev. B **89**, 125101 (2014).
[47] M. Fagotti, J. Stat. Mech. (2014) P03016.
[48] B. Wouters, J. De Nardis, M. Brockmann, D. Fioretto, M. Rigol, and J.-S. Caux, Phys. Rev. Lett. **113**, 117202 (2014).
[49] B. Pozsgay, M. Mestyán, M. A. Werner, M. Kormos, G. Zaránd, and G. Takács, Phys. Rev. Lett. **113**, 117203 (2014).
[50] M. Greiner, O. Mandel, T. Hänsch, and I. Bloch, Nature (London) **419**, 51 (2002).
[51] T. Kinoshita, T. Wenger, and D. S. Weiss, Nature (London) **440**, 900 (2008).
[52] S. Hofferberth, I. Lesanovsky, B. Fischer, T. Schumm, and J. Schiedmayer, Nature (London) **449**, 324 (2007).
[53] I. Bloch, J. Dalibard, and W. Zwerger, Rev. Mod. Phys. **80**, 885 (2008).
[54] S. Trotzky, Y.-A. Chen, A. Flesch, I. P. McCulloch, U. Schollwöck, J. Eisert, and I. Bloch, Nature Phys. **8**, 325 (2012).
[55] M. Gring, M. Kuhnert, T. Langen, T. Kitagawa, B. Rauer, M. Schreitl, I. Mazets, D. A. Smith, E. Demler, and J. Schmiedmayer, Science **337**, 6100 (2012).
[56] M. Cheneau, P. Barmettler, D. Poletti, M. Endres, P. Schaua, T. Fukuhara, C. Gross, I. Bloch, C. Kollath, and S. Kuhr, Nature (London) **481**, 484 (2012).
[57] U. Schneider, L. Hackeruller, J. P. Ronzheimer, S. Will, S. Braun, T. Best, I. Bloch, E. Demler, S. Mandt, D. Rasch, and A. Rosch, Nature Phys. **8**, 213 (2012).
[58] M. Kuhnert, R. Geiger, T. Langen, M. Gring, B. Rauer, T. Kitagawa, E. Demler, D. Adu Smith, and J. Schmiedmayer, Phys. Rev. Lett. **110**, 090405 (2013).
[59] T. Langen, R. Geiger, M. Kuhnert, B. Rauer, and J. Schmiedmayer, Nature Phys. **9**, 640 (2013).
[60] F. Meinert, M. J. Mark, E. Kirilov, K. Lauber, P. Weinmann, A. J. Daley, and H.-C. Nagerl, Phys. Rev. Lett. **111**, 053003 (2013).
[61] T. Fukuhara, A. Kantian, M. Endres, M. Cheneau, P. Schaua, S. Hild, C. Gross, U. Schollwöck, T. Giamarchi, I. Bloch, and S. Kuhr, Nature Phys. **9**, 235 (2013).
[62] J. P. Ronzheimer, M. Schreiber, S. Braun, S. S. Hodgman, S. Langer, I. P. McCulloch, F. Heidrich-Meisner, I. Bloch, and U. Schneider, Phys. Rev. Lett. **110**, 205301 (2013).
[63] S. Braun, M. Friesdorf, S. Hodgman, M. Schreiber, J. Ronzheimer, A. Riera, M. del Rey, I. Bloch, J. Eisert, and U. Schneider, arXiv:1403.7199.
[64] J. M. Deutsch, Phys. Rev. A **43**, 2046 (1991).
[65] M. Srednicki, Phys. Rev. E **50**, 888 (1994).
[66] M. Srednicki, J. Phys. A **29**, L75 (1996).
[67] M. Srednicki, J. Phys. A **32**, 1163 (1999).
[68] S. Goldstein, J. L. Lebowitz, R. Tumulka, and N. Zanghí, Phys. Rev. Lett. **96**, 050403 (2006).
[69] S. Goldstein, J. L. Lebowitz, C. Mastrodonato, R. Tumulka, and N. Zanghi, Proc. R. Soc. A **466**, 3203 (2010).
[70] S. Goldstein, J. L. Lebowitz, R. Tumulka, and N. Zanghi, Eur. Phys. J. H **35**, 173 (2010).
[71] T. N. Ikeda, Y. Watanabe, and M. Ueda, Phys. Rev. E **84**, 021130 (2011).
[72] T. N. Ikeda, Y. Watanabe, and M. Ueda, Phys. Rev. E **87**, 012125 (2013).
[73] R. Steinigeweg, J. Herbrych, and P. Prelovšek, Phys. Rev. E **87**, 012118 (2013).
[74] W. Beugeling, R. Moessner, and M. Haque, Phys. Rev. E **89**, 042112 (2014).
[75] R. Steinigeweg, A. Khodja, H. Niemeyer, C. Gogolin, and J. Gemmer, Phys. Rev. Lett. **112**, 130403 (2014).
[76] S. Sorg, L. Vidmar, L. Pollet, and F. Heidrich-Meisner, arXiv:1405.5404v2.
[77] W. Beugeling, R. Moessner, and M. Haque, arXiv:1407.2043.

[78] V. Khemani, A. Chandran, H. Kim, and S. L. Sondhi, arXiv:1406.4863.
[79] H. Kim, T. N. Ikeda, and D. Huse, arXiv:1408.0535.
[80] L. Bonnes, F. H. L. Essler, and A. M. Läuchli, arXiv:1404.4062 (2014).
[81] J.-S. Caux and J. Mossel, J. Stat. Mech. (2011) P02023.
[82] V. Alba, M. Fagotti, and P. Calabrese, J. Stat. Mech. (2009) P10020.
[83] N. Kitanine, J. M. Maillet, and V. Terras, Nucl. Phys. B **554**, 647 (1999).
[84] N. Kitanine, J. M. Maillet, and V. Terras, Nucl. Phys. B **567**, 554 (2000).
[85] L. Amico, R. Fazio, A. Osterloh, and V. Vedral, Rev. Mod. Phys. **80**, 517 (2008).
[86] M. Takahashi, *Thermodynamics of one-dimensional solvable models*, Cambridge University Press 1999.
[87] C. N. Yang and C. P. Yang, J. Math. Phys. **10**, 1115 (1969).
[88] M. Takahashi, Prog. Theor. Phys. **46**, 401 (1971).
[89] M. P. Grabowski and P. Mathieu, Ann. Phys. N.Y. **243**, 299 (1995).
[90] J. Eisert, M. Cramer, and M. B. Plenio, Rev. Mod. Phys. **82**, 277 (2009).
[91] P. Calabrese, J. Cardy, and B. Doyon Eds., Special issue: Entanglement entropy in extended systems, J. Phys. A **42**, 50 (2009).
[92] P. Calabrese and J. Cardy, J. Phys. A **42** 504005 (2009).
[93] V. E. Korepin, N. M. Bogoliubov, and A. G. Izergin, *Quantum Inverse Scattering Methods and Correlation Functions*, Cambridge University Press 1997.
[94] X. Zotos and P. Prelovšek, Phys. Rev. B **53**, 983 (1996).
[95] H. Castella and X. Zotos, Phys. Rev. B **54**, 4375 (1996).
[96] X. Zotos, F. Naef, and P. Prelovšek, Phys. Rev. B **55**, 11029 (1997)
[97] F. C. Alcaraz, M. I. Berganza, and G. Sierra, Phys. Rev. Lett. **106**, 201601 (2011).
[98] I. Pizorn, arXiv:1202.3336.
[99] M. I. Berganza, F. C. Alcaraz, and G. Sierra, J. Stat. Mech. (2012) P01016.
[100] G. Wong, I. Klich, L. A. P. Zayas, and D. Vaman, JHEP **12** (2013) 020.
[101] M. Storms, and R. R. P. Singh, Phys. Rev. E **89**, 012125 (2014).
[102] R. Berkovits, Phys. Rev. B **87**, 075141 (2013).
[103] F. H. L. Essler, A. M. Läuchli, and P. Calabrese, Phys. Rev. Lett. **110**, 115701 (2013).
[104] M. Nozaki, T. Numasawa, T. Takayanagi, Phys. Rev. Lett. **112**, 111602 (2014).
[105] G. Ramirez, J. Rodriguez-Laguna, and G. Sierra, arXiv:1402.5015.
[106] F. Ares, J. G. Esteve, F. Falceto, and E. Sánchez-Burillo, arXiv:1401.5922.
[107] Y. Huang, and J. Moore, arXiv:1405.1817.
[108] T. Pálmai, arXiv:1406.3182.
[109] J. Mölter, T. Barthel,U. Schollwöck, and V. Alba, arXiv:1407.0066.
[110] H.-H. Lai and K. Yang, arXiv:1409:1224
[111] J. Sato, B. Aufgebauer, H. Boos, F. Göhmann, A. Klümper, M. Takahashi, and C. Trippe, Phys. Rev. Lett. **106**, 257201 (2011).
[112] M. Fagotti and P. Calabrese, Phys. Rev. A **78**, 010306 (2008).
[113] V. Gurarie, J. Stat. Mech. (2014) P02014.
[114] M. Collura, M. Kormos, and P. Calabrese, J. Stat. Mech. (2014) P01009.
[115] M. Kormos, L. Bucciantini, and P. Calabrese, EPL **107**, 40002 (2014).
[116] J.-S. Caux and J.-M. Maillet, Phys. Rev. Lett. **95**, 077201 (2005).
[117] J.-S. Caux, R. Hagemans and J.-M. Maillet, J. Stat. Mech. P09003 (2005).
[118] J.-S. Caux, J. Math. Phys. **50**, 095214 (2009).